

LA-UR- 09-02300

Approved for public release;
distribution is unlimited.

Title: Application of Commercial Sensor Manufacturing Methods
for NOx/NH3 Mixed Potential Sensors for Emissions Control

Author(s):
Eric L. Brosha
Rangachary Mukundan
Mark Nelson
Praveen Sekhar
Todd Williamson
Fernando H. Garzon

Intended for: 34th Technical Conference on Clean Coal
Clearwater, FL
May 31-June4, 2009



Los Alamos National Laboratory, an affirmative action/equal opportunity employer, is operated by the Los Alamos National Security, LLC for the National Nuclear Security Administration of the U.S. Department of Energy under contract DE-AC52-06NA25396. By acceptance of this article, the publisher recognizes that the U.S. Government retains a nonexclusive, royalty-free license to publish or reproduce the published form of this contribution, or to allow others to do so, for U.S. Government purposes. Los Alamos National Laboratory requests that the publisher identify this article as work performed under the auspices of the U.S. Department of Energy. Los Alamos National Laboratory strongly supports academic freedom and a researcher's right to publish; as an institution, however, the Laboratory does not endorse the viewpoint of a publication or guarantee its technical correctness.

Application of Commercial Sensor Manufacturing Methods for NO_x/NH₃ Mixed Potential Sensors for Emissions Control

Eric L. Brosha*, Rangachary Mukundan, Mark Nelson, Praveen Sekhar, Todd Williamson, and Fernando H. Garzon

Los Alamos National Laboratory

Sensors and Electrochemical Devices Group, MS D429

Los Alamos, New Mexico 87545

*Principal presenter, brosha@lanl.gov, (505) 665-4008, (505) 665-4292 (fax)

ABSTRACT

The purpose of this research effort is to develop a low cost on-board Nitrogen Oxide (NO_x)/Ammonia (NH₃) sensor that can not only be used for emissions control but has the potential to improve efficiency through better monitoring of the combustion process and feedback control in both vehicle and stationary systems. Over the past decade, Los Alamos National Laboratory (LANL) has developed a unique class of electrochemical gas sensors for the detection of carbon monoxide, hydrocarbons, hydrogen and nitrogen oxides. These sensors are based on the mixed-potential phenomenon and are a modification of the existing automotive lambda (oxygen) sensor and have the potential to meet the stringent sensitivity, selectivity and stability requirements of an on-board emissions/engine control sensor system.

The current state of the art LANL technology is based on the stabilization of the electrochemical interfaces and relies on an externally heated, hand-made, tape cast device. We are now poised to apply our patented sensing principles in a mass production sensor platform that is more suitable for real world engine-out testing such as on dynamometers for vehicle applications and for exhaust-out testing in heavy boilers/SCR systems in power plants. In this present work, our goal is to advance towards commercialization of this technology by packaging the unique LANL sensor design in a standard automotive sensor-type platform. This work is being performed with the help of a leading US technical ceramics firm, utilizing commercial manufacturing techniques. Initial tape cast platforms with screen printed metal oxide and Pt sensor electrodes have shown promising results but also clearly show the need for us to optimize the electrode and electrolyte compositions/morphologies and interfaces of these devices in order to demonstrate a sensitive, selective, and stable NO_x sensor.

Our previous methods and routes to preparing stable and reproducible mixed potential sensors – in bulk, tape cast, and thin film variants- need to be adapted as a necessary adjunct to address materials challenges resulting from the implementation of commercial manufacturing methods. We also modified the electrodes to demonstrate a NH₃ sensor that can be used in conjunction with the NO_x sensor for feedback control of emissions systems. Once desirable properties are achieved, we will work closely with potential customers in order to dynamometer and boiler test these devices. Ultimately, this will accurately gauge the level of readiness of mixed potential sensor technology for commercialization and eventual use of this important electrochemical technology.

Technical Session Topic: Advanced Controls

INTRODUCTION

There is a renewed desire to pursue the development of new and innovative sensors and control systems to support the full-scale implementation and operation of highly efficient, near-zero emission power generation systems. Sensors and process controls are vital to achieving and assuring highly efficient operation and reduced emissions. Applicable sensing technologies and transduction mechanisms available for fossil energy applications are limited because of the harsh operating conditions (e.g as defined by high temperature, dynamic pressure ranges, fuel/exhaust gas composition, etc.) and this is particularly true for *in situ* operation more so than when compared to extractive approaches.

Over the past decade Los Alamos National Laboratory (LANL) has developed a unique class of electrochemical gas sensors for the detection of carbon monoxide, hydrocarbons, hydrogen and nitrogen oxides.¹⁻¹⁶ These sensors are based on the mixed-potential phenomenon and are a modification of the existing automotive lambda (oxygen) sensor and have the potential to meet the stringent sensitivity, selectivity and stability requirements of an on-board emissions/engine control sensor system.¹⁷⁻²⁴ The current state of the art LANL technology is based on the stabilization of the electrochemical interfaces and relies on an externally heated device that is fabricated using ceramic tape-casting methods.¹⁶⁻²⁵ This prior work has placed us in an excellent position to utilize our patented sensor configuration to create a prototype sensor that emphasizes more the commercial attributes making it suitable for *in situ* testing in heavy boilers and for mass production in general. In this project, we employed commercial sensor manufacturing techniques with the goal to move this technology from an externally heated, extraction-based system (suitable for laboratory R&D) towards a prototype device more suitable for commercialization. New sensors have been prepared that incorporate the unique LANL sensor design in a planar, self-heated, automotive sensor-type platform. This configuration will facilitate device testing under conditions that are more representative of a real world environment for clean coal combustions applications as well as for engine out applications for both vehicle and stationary uses.

In this work, we found that we were able to successfully demonstrate a mixed potential sensor fabricated using mass-production tape casting and screen-printing methods. The LANL approach to mixed potential sensors is compatible with most aspects of the state-of-the-art fabrication methods presently used by automotive sensor manufacturers. The principal remaining and unresolved issue at the conclusion of this study is whether the sensor's YSZ solid electrolyte can be screen-printed and co-fired with the sensor body and electrodes and whether the properties of the screen-printed electrolyte can be optimized to duplicate the sensor behavior already seen in laboratory devices.^{1-4, 14, 15, 25}

EXPERIMENTAL

The materials selection and processing of LANL tape cast mixed potential sensors has been presented in detail elsewhere.^{1,2,11,26,27} Sr-doped lanthanum chromite was selected as the working electrode and Pt was selected as the pseudo-reference, counter electrode since we demonstrated that this electrode pair produced a total NO_x sensor with desirable sensor characteristics in earlier work.¹⁴ Drawing schematics of the proposed commercial planar sensors were designed at LANL and sent to ElectroScience Laboratories (ESL, King of Prussia, PA).

The dimensions were selected so that they match or easily scale to existing automotive packaging designs for a flat plate O₂ sensors. The dimensions were the anticipated values after-firing and densification of the ceramic tape since significant shrinkage accompanies any high temperature firing of a ceramic component. ESL compensated for this shrinkage factor when preparing all of the layers of screen-printing masks necessary to prepare a final green-body in a single firing. The sensor body was fabricated using unfired, alumina tape cast green body that had the electrodes and Pt leads and resistive heater screen-printed onto the surfaces in subsequent steps. The entire device was then co-fired using a proprietary, multi-step schedule.

Figure 1 is a digital photograph of one of the first LANL NO_x sensors prepared showing the reverse heater side and the sensors' critical working and counter electrodes and the YSZ electrolyte.

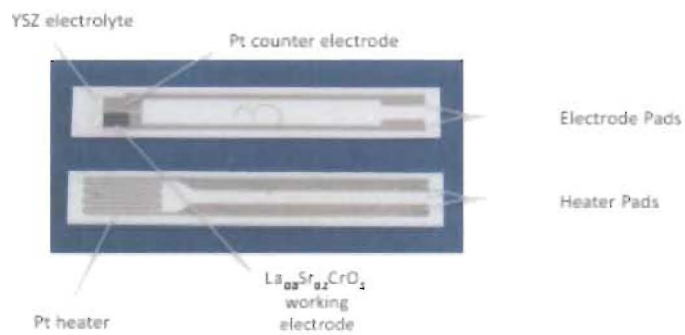


Figure 1. Photograph of an ESL-prepared NO_x automotive-style sensor utilizing unique LANL mixed potential sensor architecture.

A new sensor testing apparatus was prepared that was a departure from the hot-walled, laboratory tube furnace approach used in our previous sensor R&D. In the past, a sensor was placed in the center of an externally heated quartz tube with gas tight fittings placed at either end. This experimental configuration was not necessary since the ESL-prepared sensors incorporated a resistive Pt heater. Figure 2 is a photograph of a specially prepared quartz tube that placed the sensor electrodes in the test gas stream in a manner not too unlike the orientation that commercial automotive sensors are placed in an exhaust manifold of a vehicle or engine dynamometer. A commercial flat-plate O₂ sensor mount was used to hold the LANL sensor using the four metal spring-loaded clips that would normally be used with a commercial sensor. A rubber stopper was used to hold the packaging in place and silicone gasket sealant was used to seal the gaps around the four wires providing electrical contact to the sensor electrodes and heater.

RESULTS AND DISCUSSION

Figure 3 shows the heater resistance as a function of temperature as external heat was applied to the device. The sensor body was then removed from the tube furnace and placed into the cold-walled test cell with a thermocouple affixed to the electrode region of the sensor with Ag epoxy. Figure 3 also shows sensor electrode temperature as a function of applied heater voltage. The heater power is plotted with knowledge of both heater voltage and heater current. The resistance

tolerances of the Pt thin films were quite good with one group of the first batch of sensors having an average resistance of 9 ohms with a standard deviation of 5%.

The room temperature, two-point resistance across various points of the electrodes was measured on several devices. The two-point resistance from the Pt pad to the Pt counter electrode was typically about 2.9 - 3.0 ohms. We suspect that much of this resistance is contact resistance.

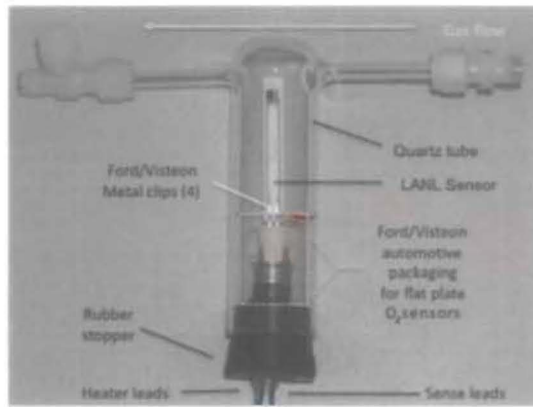


Figure 2. Photograph of the testing apparatus created for the new automotive-style NO_x sensor. Standard, automotive, flat-plate ceramic sensor packaging was modified and demonstrates compatibility of the new LANL device with present, commercial sensor packaging.

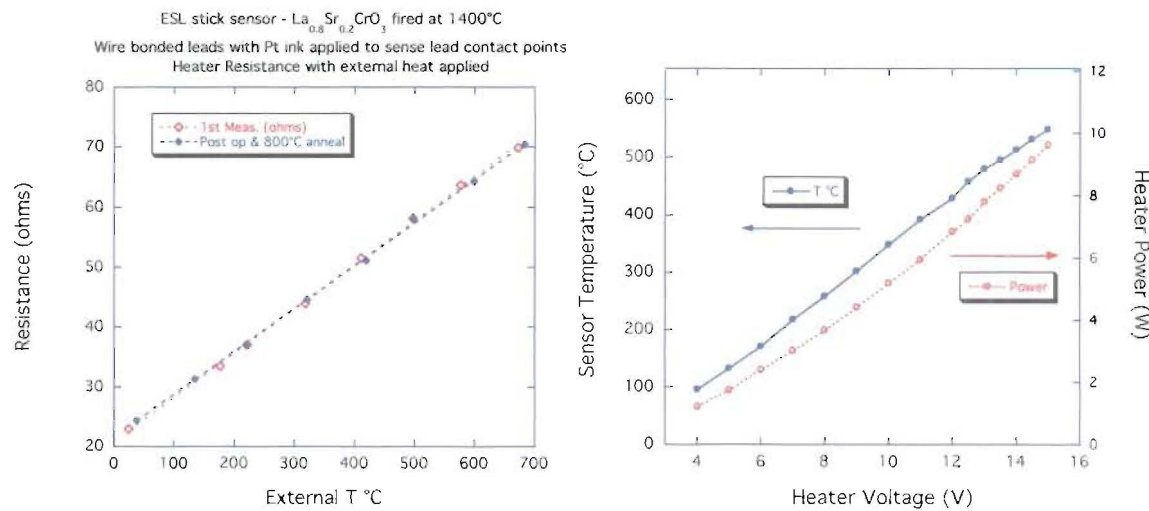


Figure 3. Initial samples provided to us from ESL permitted the testing of the resistive Pt thin film heater. (Left) The heater resistance was determined as a function of temperature as delivered and after an extended 800°C anneal. The heater resistance may be used by control electronics for temperature feedback. (Right) Measurement of electrode/electrolyte temperature and heater power as a function of applied voltage.

The two-point resistance for the lanthanum-chromite working electrode, measured in an identical fashion, was substantially higher as predicted due to the much lower electronic

conductivity of the metal oxide. The average resistance of the chromite electrodes was on the order of 55-75 K-ohms. All of these values are not unreasonable based on previous, bulk sensor work. Nevertheless, controlling and tailoring these values will be important for future device optimization.

Several sensors were chosen at random from the first batch of ESL devices. The difference between the devices was a slight difference in target porosity/density of the YSZ solid electrolyte, a difference that could readily be discerned with the unaided eye. All of the initially tested devices functioned and produced a measureable response to CO, HCs, NO_x and hydrogen species. The interference from CO and H₂ were minimal and were not studied after initial measurements were made. The test fixture worked very well as little noise was seen in the data although the large dead space surrounding the shaft of the sensor undoubtedly lead to increased response times. The response times are in part controlled by the flow rate of the air across the sensor and 200 sccm was used for these experiments and was limited by the experimental setup. The left plot in Figure 4 is a typical response of the devices tested in open circuit (un-biased mode) for 100 ppm of NO, 100 ppm of NO₂, 500 ppm of C₃H₆ and 500 ppm of C₃H₈.^{14,25,27} All of the devices except one produced a similar unbiased response. One device produced little response to any test gas at any operating voltage. A closer inspection under an optical microscope revealed that the source of this anomalous behavior of this one device was caused by a small crack bisecting the electrolyte between the working and counter electrodes.

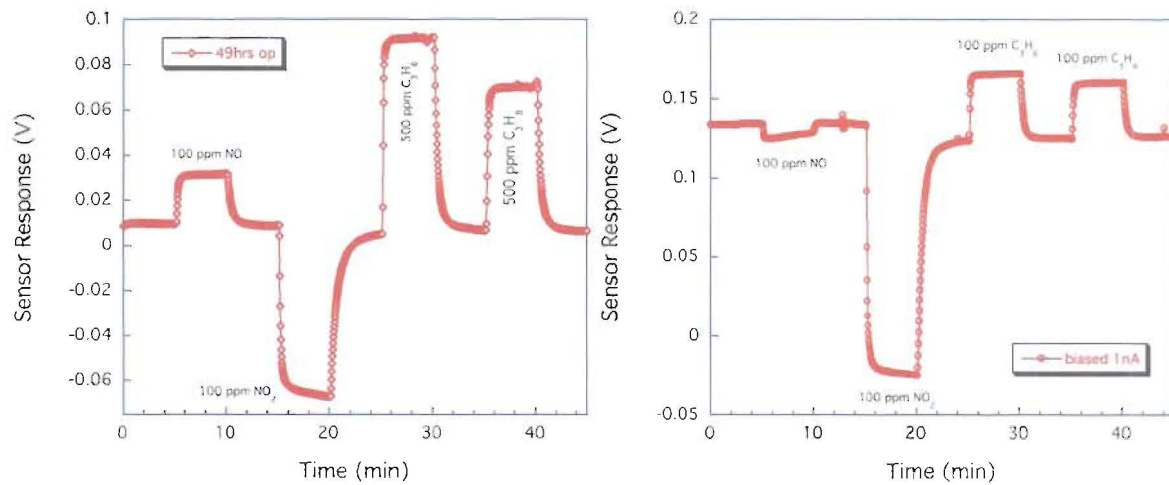


Figure 4. Response of ESL device 1A#4 using Pt resistive heater to 100 ppm NO, 100 ppm NO₂, 500 ppm C₃H₆, and 500 ppm C₃H₈ in an air background flowing at 200 sccm for open circuit (Left) and current biased conditions (1nA applied current, Right). Heater voltage and current was 14.03V and 0.63A.

In the next experiment, a current bias was applied to study how the relative HC/NO_x sensitivity changed under applied current bias. Figure 4 also shows the change in the response characteristics of one of the ESL devices to 1nA of applied current. The right-hand plot in Figure 4 shows several characteristics that we saw with the bulk, tape-casted laboratory sensors in that the NO response turns negative (as is the case with the NO₂ signal) and the HC response is reduced.^{14,25,27} This phenomenon is a result of a resistance change superimposed upon the mixed potential generated by the presence of the test gas. The magnitude of the resistance change is a

function of the electrode/electrolyte interface in the presence and absence of NO_x/HCs . The current biased behavior seen for LANL-prepared tape cast devices differs than what is seen in Figure 4. Figure 5 shows the unbiased and biased response of a large, externally heated tape cast device prepared for this work to study in comparison to the ESL devices and agrees very well to previous work.¹⁴ The fact that the behavior of the ESL devices differs from previous bulk-type LANL devices was not unexpected and merely suggests that further optimization of the planar devices will be required.

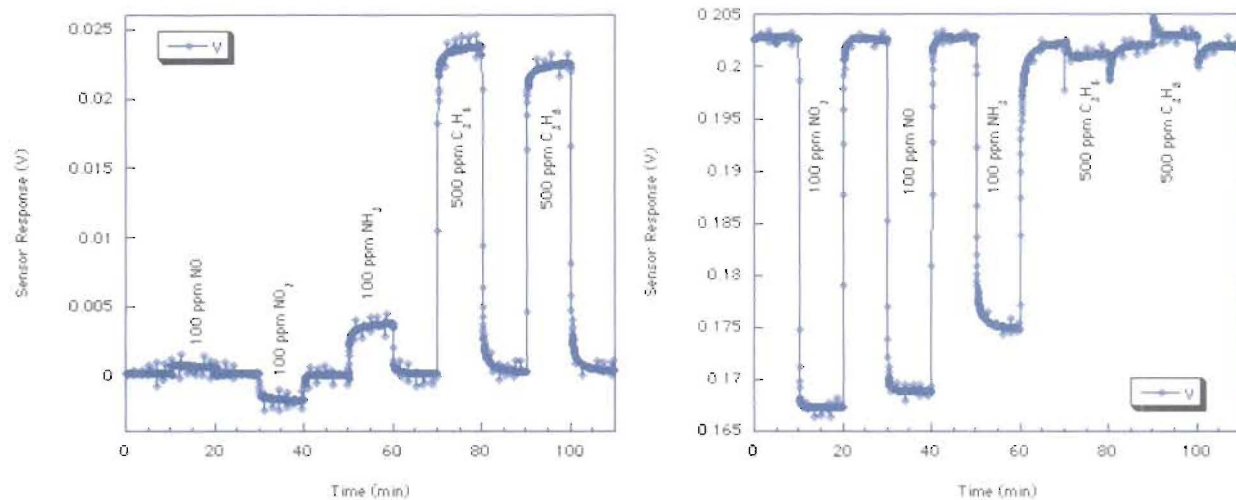


Figure 4. Response of a LANL-prepared tape cast, LaSrCrO/YSZ/Pt device operating at 550°C (externally heated in tube furnace) to 100 ppm NO, 100 ppm NO_2 , 500 ppm C_3H_6 , and 500 ppm C_3H_8 in an air background flowing at 200 sccm for open circuit (Left) and current and at 1 μA current bias (Right).

The device that produced the response data shown in Figure 4 was selected for a lifetime test. This device was operated continuously in one test fixture over a period of almost 700 hours while periodically open circuit and biased measurements were made. Our previous NO_x sensor work showed that any sensor aging is quickly apparent, as the baseline voltage under current bias is sensitive to small changes in device impedance. Such changes in total device impedance may be the result of interfacial reactions due to impurities, chemical reaction between electrode/electrolyte phases, or changes in electrode/electrolyte morphology.

Figure 5 shows the reduced data from these series of experiments. For each run, 100 ppm levels of NO and NO_2 were compared to 500 ppm levels of propane and propylene. The open circuit data shows little drift; however the biased results clearly show a problem in terms of device response stability. The voltage level for 100 ppm NO_2 shows the most change over time. The absolute level of voltage produced for 100 ppm NO does increase over time however it is nowhere near the level of voltage for the 100 ppm NO_2 . The hydrocarbons are not stable over time as well. Under biased conditions, the measured voltage is a superposition of the mixed potential voltage and the voltage need to maintain a constant current. The drift in sensor response was not observed in the LANL bulk devices utilizing controlled interfaces and therefore must be an artifact of the use of commercial ceramic processes. Since it was apparent as early as 150 hours that the ESL device was showing signs of aging, other samples were studied to determine a cause.

Post-mortem analyses of the ESL sensors was performed using electron microscopy (SEM and ESEM) and x-ray analytical techniques. Figure 6 is an SEM image of the doped lanthanum chromite electrode. This electrode was prepared by screen-printing ink using powdered $\text{La}_{0.8}\text{Sr}_{0.2}\text{CrO}_3$ that was purchased from Praxair. It is well known from extensive solid oxide fuel cell research that it is difficult to sinter chromium oxide phases below about 1600°C which has led to novel methods to prepare dense lanthanum chromite materials and films.^{28,29} The screen-printed films prepared by ESL appear to be adequate for our sensors. While film shows porosity, the chromite particles are well sintered showing a relatively smooth surface, good cohesion, and good adhesion with the alumina substrate.

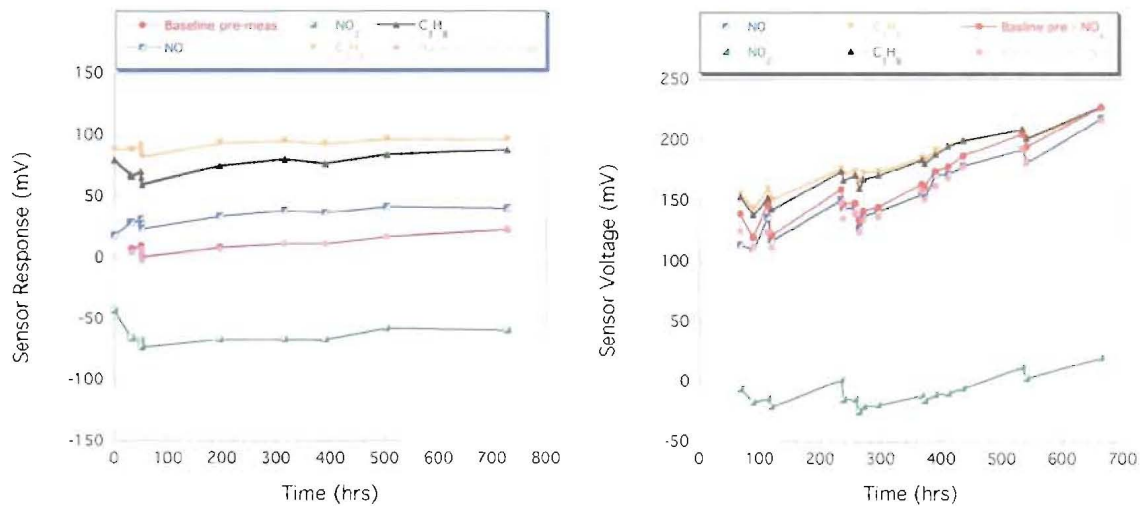


Figure 5. Long term, isothermal test data for 1A#4 over 700 hours of continuous operation at open circuit (Left) and 1nA biased (Right). Open circuit stability indicates steady heater performance and unchanging heterogeneous catalytic properties, the large drift in the biased sensor voltage is symptomatic of changes in the ionic conductivity of the electrolyte or charge transfer resistance of the electrode/electrolyte interface.

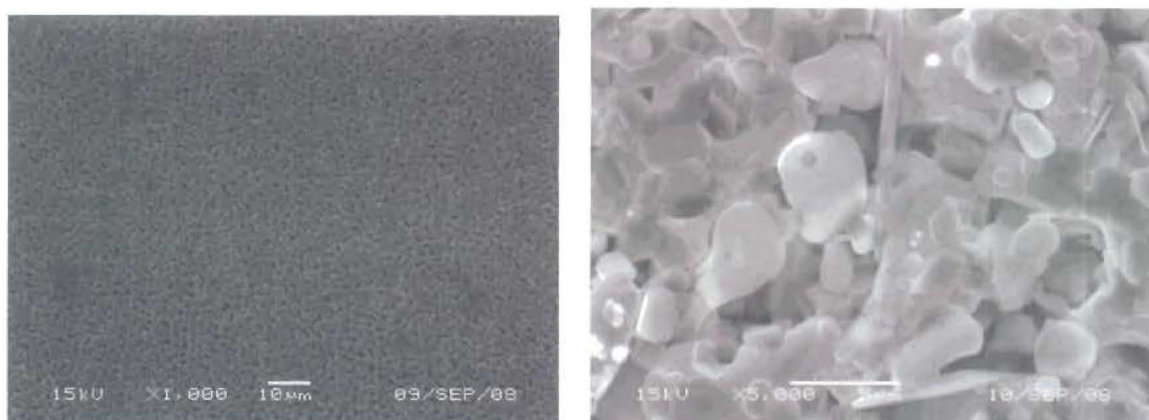


Figure 6. (Left) SEM micrograph of the $\text{La}_{0.8}\text{Sr}_{0.2}\text{CrO}_3$ screen-printed working electrode after firing and densification. (Right) SEM micrograph of the ESL screen-printed Pt counter electrode shows a rough surface with a large particle size distribution and random morphology.

The Pt counter electrode has some undesirable attributes compared to the chromite electrode. The uniformity seen in the metal-oxide, working electrode is absent. There is a large distribution of Pt grain sizes and shapes and, unlike the chromite electrode, the surface is more rough. This roughness will produce an electrode/electrolyte interface with a high surface or electro-active area and this is the exact opposite of what our previous mixed potential research has shown is desirable. Furthermore, some sensors showed a Pt counter electrode with needle-like grain structure. Moreover, such grains produce an interface with a high surface energy and as such, structures with this morphology are prone to grain growth at elevated temperature. This is unwanted in a mixed potential sensor since it will cause a change in device response with time. Therefore, the Pt electrode must be improved – both in terms of uniform grain structure and smoothness – in order to make these devices into successful mixed potential NO_x sensors using commercial methods.

After completion of the 700 hr life test, the device was studied using 3-dimensional, X-ray tomography (MicroXCT™, xradia Corp.). The use of X-ray imaging tomography has allowed us to see the structure of the device underneath the YSZ electrolyte at the electrode/electrolyte interface. It is this interface that governs the sensor response behavior and is responsible for any aging characteristics. Inspection of Figure 7 immediately shows some interesting results that can easily explain the aging phenomena during the life test. First, and most obvious, is the crack surrounding the chromite working electrode. This crack was not apparent to the unaided eye. Second, there is a large population of pinhole defects surrounding both electrodes. These defects are most likely caused by the screen-printing and masking process and their presence will affect YSZ adhesion, thermal expansion properties, and mechanical stability and will be the source of more cracks and ultimately lost adhesion commensurate with thermal cycling. Lastly, there are several substantial defects along the Pt/solid electrolyte interface and this placement could easily explain the large amount of drift in sensor baseline voltage since this is an area where the current flow could easily be affected. Also, the high degree of roughness of the Pt electrode can be seen in the upper right image in Figure 7.

Some of the remaining companion samples were examined to determine the strength of the adhesion of the YSZ electrolyte to the underlying electrodes and alumina substrate. It was found that very little force was needed to break the YSZ layer away from the electrodes and alumina substrate. With the first series of sensors, a portion of the screen-printed YSZ layer covered the Pt and chromite electrodes and a portion of the alumina substrate. The stresses induced on the YSZ layer, brought about by the simultaneous contact with materials of different thermal expansion coefficients, may have weakened the adhesion of the electrolyte to the electrode materials. Analysis showed that the underlying electrodes show no sign of damage or evidence of adhesion to the YSZ and this suggests little interaction between the electrode and electrolyte during the sintering and densification process.

We provided feedback to ESL on all of these issues. ESL altered several processing parameters and prepared a new series of devices where the screen-printed process used on the YSZ layer was changed to mitigate the defects. The open circuit response of these devices behaved similarly to the previous batches however the current biased response behaved poorly as with the first series. X-ray tomography analysis of one of the new devices showed that there was a discontinuity in thickness and YSZ morphology at the transition point from the alumina body onto the Pt electrode confined to the region between the two electrodes. This explains why the current biased performance was no better in these devices compared to the first sensor series.

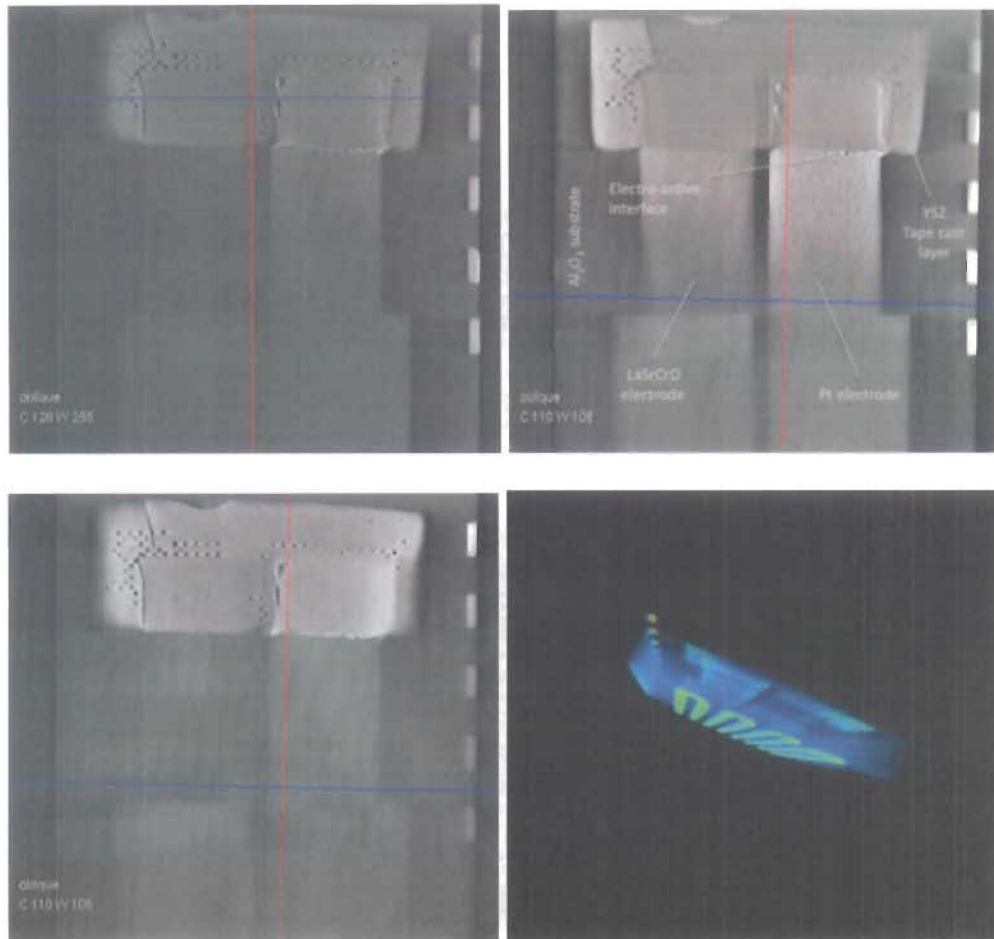


Figure 7. Micro-XTC™ tomography imaging of an ESL prepared NO_x sensor with La-Sr-Cr-O working electrode, Pt counter electrode, and YSZ electrolyte in three different image planes and contrast values (top left and right, bottom left) and a false-color composite image showing patterned Pt resistive heater (bottom right) and working sensor structures from the bottom perspective. Defects in the YSZ solid electrolyte – including large cracks- are clearly seen in these images.

The irregular morphology of the Pt electrode and the rough surface may have affected the morphology of the overcoat YSZ and this may have contributed to the interfacial damage seen on many of the sensors. Reformulated Pt ink was prepared and the firing temperature modified to create a smoother, denser Pt electrode. Figure 8 shows SEM micrographs of an improved ink formulation after trying a few new formulations and firing temperatures. The new ink shows a more uniform grain size and an overall smoother microstructure with less porosity. This is illustrated in the figure where there is little porosity with smaller grains populating the surface on top of large, 10-20 μm sized Pt grains. Also, profilometer data or surface roughness data of the sample show an improvement vis-à-vis a smoother Pt film. The testing of ESL-prepared sensors with the new smooth, dense Pt electrode will be the focus of future work.

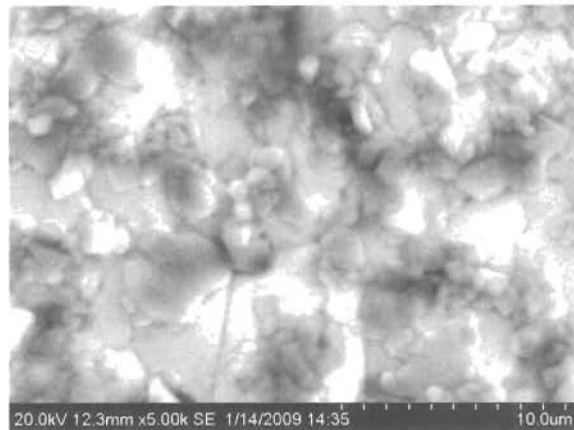


Figure 8. SEM Micrographs of post-fired ESL Pt ink used for the LANL devices. The old formulation fired at 1450°C for 1.5hr is in the images on the Left compared to images of the new ink formulation fired at 1510°C on the Right.

Ammonia Sensor Development Using Modified ESL NO_x Sensors

As a result of earlier work, we have tested and have filed a patent application for mixed potential sensor of the LANL configuration (tape cast configuration with Au and Pt wires as stable, reproducible electrodes) for ammonia.³⁰ In previous work we prepared a tape cast device that utilized a stable Au wire electrode in place of the strontium-doped lanthanum chromite working electrode. It was not possible to prepare a device analogous to the planar NO_x sensor since the low melting point of gold precludes firing the Au electrode along with the sensor body. Furthermore, the low melting point also precluded the screen-printing and firing of the YSZ electrolyte in a two-step process. The YSZ may be deposited using a vapor deposition approach, a method that is routinely used in industry for optical coatings and even to apply Pt electrodes on YSZ electrolyte for automotive sensors. We did prepare a few ammonia sensors at LANL using modified ESL-prepared NO_x sensors. We removed the Pt and lanthanum chromite electrodes and applied Au/Pt electrodes using RF sputtering.

Figure 9 (Left) is the open circuit response of an ESL prepared device (a companion device to the one that produced the NO_x/HC response in Figure 4) including testing with 100 ppm of NH₃. As with our earlier, tape cast devices (e.g. like the response shown in Figure 5), the sensor shows a positive (ammonia oxidation) response when operated in an open circuit mode; comparable but opposite in sign to the voltage produced with 100 ppm of NO₂. As with the other ESL-prepared, LANL mixed potential devices, the sensor did not respond in the manner of a tape casted sensor under current bias because of the properties of the screen-printed YSZ, ESL-applied electrolyte.

In the last experiment of this project, we utilized a heated ESL substrate without a working electrode or the electrolyte. We sputter-deposited an un-optimized Au working electrode film (5000 Å) in place of the chromite, metal oxide electrode used for the NO_x sensors. Figure 9 (Right) shows the preferential response to NH₃ versus NO₂ and establishes a proof of concept that ESL will be able to fabricate these devices in the automotive “stick” platform. The properties of the sensor that produced Figure 9 are completely un-optimized and are the result of standard deposition parameters used for previous LANL thin film sensor work. However, the preferential sensitivity of a device utilizing a stable Au electrochemical interface to ammonia is

demonstrated. These results, taken together with a LANL grown YSZ electrolyte, demonstrate the potential to commercialize both the NO_x sensor and NH_3 sensor.

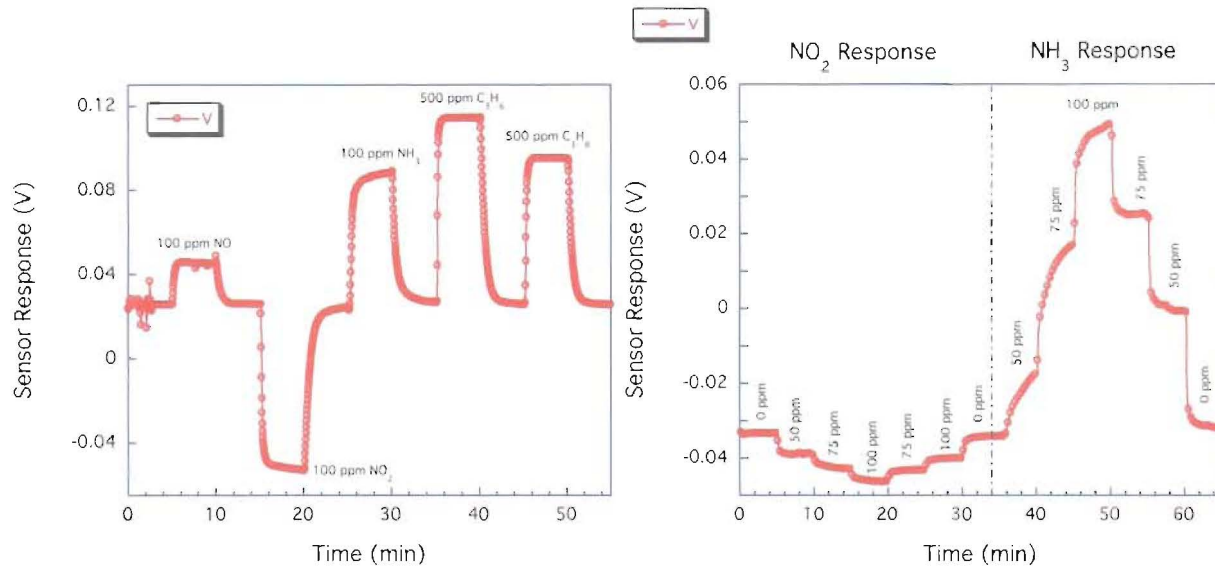


Figure 9. (Left) ESL Device 1A #3 operated at 15V and 0.62A in 200 sccm of air and response to 100 ppm NO, NO_2 , NH_3 , and 500 ppm C_3H_6 and C_3H_8 . (Right) ESL Device 3#6 with an un-optimized LANL sputtered Au working electrode and LANL sputtered YSZ electrolyte operated at 6.8V and 0.70A in 200 sccm of air and response to NO_2 and NH_3 showing a large preferential sensitivity to ammonia.

CONCLUSIONS

We implemented designs for a new mixed potential NO_x sensor that incorporates the ideal properties unique to the LANL methodology, selected electrode materials, and had a sensor prototyping facility (ESL ElectroScience Laboratories of King of Prussia, PA) provide us commercially prepared sensors for our evaluation. The challenge of this work was to preserve the electrochemical and interfacial properties unique to LANL mixed potential sensors using manufacturing methods presently in use for automotive combustion control sensors. Overall, this project was successful in that most of the devices functioned as a mixed potential gas sensor in the open circuit mode. We studied the materials properties of the electrodes (electronic conductivity, adhesion to substrate, cohesion, micro-structure, etc.), the YSZ electrolyte, and most importantly, the microstructure of the electrode/solid electrolyte interface. We found that the lanthanum chromite electrode possessed adequate adhesion, cohesion, and electronic conductivity for use as a mixed potential sensor. The original Pt electrode suffered from high surface roughness and a high surface energy morphology that would account for the aging problems. A new ink and firing schedule has been developed.

The sensor response to NO, NO_2 , and HC cross interferents was studied in open circuit and in biased modes for up to 700 hours of continuous operation. We also studied heater performance, mechanical stability to thermal cycling, and overall device stability. The devices exhibited exceptional mechanical stability and showed very little effects of aging in open circuit

(predominant hydrocarbon mode). However, response drift was seen in the current biased mode used to augment sensitivity to NO_x . Furthermore, the device response characteristics in biased mode did not behave like LANL tape cast NO_x sensors we have studied in the past. An analysis conducted on the morphology using scanning electron microscope (SEM) and environmental scanning electron microscope (ESEM) methods showed that these negative performance attributes were caused by poor electrolyte film attributes and by the presence of physical defects in the YSZ electrolyte and particularly at the electrode/electrolyte interface. This materials property issue must be addressed in future work.

REFERENCES

1. R. Mukundan, E. L. Brosha, and F.H. Garzon, US Pat. #6,605,202 (2003).
2. F.H. Garzon R. Mukundan and E.L. Brosha, US Pat. #6,656,336 (2003).
3. F.H. Garzon R. Mukundan and E.L. Brosha, US Pat. # 7,214,333(2007).
4. F. H. Garzon, R. Mukundan, and E.L. Brosha, US Pat. #7,264,700 (2007).
5. R, Mukundan, Eric L. Brosha, David R. Brown, and Fernando H. Garzon, *Electrochem. Solid-State Let.* **2** (8) (1999) 412-414.
6. Fernando H. Garzon, Rangachary Mukundan, and Eric L. Brosha, *Solid State Ionics* **136-137** (2000) 633-638.
7. E. L. Brosha, R. Mukundan, D. R. Brown, F. H. Garzon, J. H. Visser, M. Zanini, Z. Zhou, and E. M. Logothetis, *Sensors and Actuators B* **69**(#1-2) (2000) 171-182.
8. R. Mukundan, E. L. Brosha, D. R. Brown, and F.G. Garzon, *J. Electrochem. Soc.* **147** (4) (2000) 1583-1588.
9. Eric L. Brosha, Rangachary Mukundan, David R. Brown, and Fernando H. Garzon, *Solid State Ionics* **148** (2002) 61-69.
10. Eric L. Brosha, Rangachary Mukundan, David R. Brown, and Fernando H. Garzon, *Sensors and Actuators B* **87** (2002) 47-57.
11. Rangachary Mukundan, Eric L. Brosha, and Fernando H. Garzon, *J. Electrochem. Soc.* **150** (12) H2799-H284 (2003).
12. Fernando H. Garzon, Eric L. Brosha, and Rangachary Mukundan, *Solid State Ionics* **175** (2004) 487-490.
13. Eric L. Brosha, Rangachary Mukundan, Roger Lujan, Fernando H. Garzon, *Sensors and Actuators B* **119** (2006) 398-408.

14. Rangachary Mukundan, Kazuhiro Teranishi, Eric L. Brosha, and Fernando H. Garzon *J. Electrochem. Soc. Lett.* **10** (2) (2007) J26-J29.
15. Rangachary Mukundan, Eric L. Brosha, Fernando H. Garzon, Robert Novak, and Rick Soltis, Transactions of the 210th Meeting of the Electrochemical Society, **3** no. 10, October 2006, Cancun Mexico.
16. Eric L. Brosha, Rangachary Mukundan, Roger Lujan, and Fernando H. Garzon, ESC Transactions for the 214th Meeting of the ECS, Honolulu, HI, October 2008.
17. W. J. Flemming, *J. Electrochem. Soc.*, **124**, 21 (1977).
18. D. E. Williams, P McGeehin and B. C. Tofield, in Solid State Chemistry, R. Metselaar, H. J. M. Heijlingers and J Schoonman, Editors, Proc. Second European Conf. Solid State Chemistry, Veldhoven, The Netherlands, June 7-9, p. 275 (1982).
19. A. R. Pebler, US Patent 4,005,001 (1977).
20. N. Miura, T. Raisen, G. Lu, and N. Yamazoe, *J. Electrochem. Soc.*, **144**, L198 (1997).
21. T. Hibino, Y. Kuwahara, S. Wang, S. Kakimoto, and M. Sano, *Electrochem. and Solid State Lett.*, **1**(4), 197 (1998).
22. Y. Nakanouchi, H. Kurosawa, M. Hasei, Y. Yan, and A. Kunimoto, *SAE Paper 961130*, 11 (1996).
23. A. D. Brailsford, and E. M. Logothetis, *Sensors and Actuators*, **B52**, 195 (1998).
24. A. D. Brailsford, M. Yussouff, E. M. Logothetis, *Sensors and Actuators*, **B35-36**, 392 (1996).
25. R. Mukundan, E.L. Brosha, and F.H. Garzon, "Tape Cast Sensors and Method for Making," US Pat Appl., DOE Docket # S104,887.
26. R. Mukundan, E. Brosha, and F.H. Garzon, in Chemical and Biological Sensors and Analytical MethodsII, M. Butler, P. Vanysek, and N. Yamazoe, Editors, PV 2001-18, p. 464, The Electrochemical Society Proceedings Series, Pennington, NJ (2001).
27. Eric L. Brosha, Rangachary Mukundan, and Fernando H. Garzon, "YSZ-Based Electrochemical Sensors for Coal-Fired Combustion Control Applications," 33rd International Technical Conference on Coal Utilization, Clearwater FL, June 1-5, 2008.
28. Eric L. Brosha, Rangachary Mukundan, Fernando H. Garzon, proceedings of the 201st meeting of the Electrochemical Society, Philadelphia. May 2002.
29. Eric L. Brosha, Rangachary Mukundan, David R. Brown, Q. X. Jia, Roger Lujan, and Fernando H. Garzon, *Solid State Ionics* **166** (2004) 425-440.

30. R. Mukundan, E. Brosha, and F. Garzon, "Ammonia and Nitrogen Oxide Sensors," US Pat. Applied for, DOE Docket# S112,823.

ACKNOWLEDGMENTS

We wish to thank the DOE and Roland Gravel of the office of Vehicle Technologies for providing funding for this work. We would also like to acknowledge the contributions of other sources of LANL sensor funding over recent years including DOE Hydrogen Programs and LANL Tech Transfer and Royalty funds.